Improved evaluation of the next-next-to-leading order QCD corrections to e^+e^- annihilation into hadrons

Piotr A. Rączka* and Andrzej Szymacha

Institute of Theoretical Physics, Department of Physics, Warsaw University, ul. Hoża 69, PL-00-681 Warsaw, Poland

The next-next-to-leading order QCD corrections to e^+e^- annihilation into hadrons are considered. The stability of the predictions with respect to change of the renormalization scheme is discussed in detail for the case of five, four, and three active quark flavors. The analysis is based on the recently proposed condition for selecting renormalization schemes according to the degree of cancellation that they introduce in the expression for the scheme-invariant combination of the expansion coefficients. It is demonstrated that the scheme dependence ambiguity in the predictions obtained with the conventional expansion is substantial, particularly at lower energies. It is shown, however, that the stability of the predictions is greatly improved when QCD corrections are evaluated in a more precise way, by utilizing the contour integral representation and calculating numerically the contour integral. [S0556-2821(96)04123-9]

PACS number(s): 12.38.Cy, 13.60.Hb

I. INTRODUCTION

In a series of recent papers [1–5] a method has been presented for a systematic analysis of the renormalization scheme (RS) ambiguities in the next-next-to-leading (NNLO) perturbative QCD predictions. It was emphasized in [1–3] that in addition to giving predictions in some preferred renormalization scheme one should also investigate the stability of the predictions when the parameters determining the scheme are changed in some acceptable range. The method discussed in [1–3] involves a specific condition that allows one to eliminate from the analysis the renormalization schemes that give rise to unnaturally large expansion coefficients. The condition on the acceptable schemes is based on the existence in NNLO of the RS-invariant combination of the expansion coefficients, which is characteristic for the considered physical quantity. The method of [1–3] has been applied to the QCD corrections to the Bjorken sum rule for the polarized structure functions [3] and to the QCD corrections to the total hadronic width of the τ lepton [1,2,4].

In this work we apply this method to the QCD correction to $R_{e^+e^-}$ ratio:

$$R_{e^+e^-} = \frac{\sigma_{\text{tot}}(e^+e^- \to \text{hadrons})}{\sigma_{\text{tot}}(e^+e^- \to \mu^+\mu^-)}, \qquad (1)$$

which received considerable attention in recent years [6–27]. We show that a straightforward application of the condition proposed in [1–3] to the conventional perturbative expression for the QCD effects in the $R_{e^+e^-}$ ratio exhibits a rather strong RS dependence, even at high energies. Looking for improvement and motivated by the analysis of the corrections to the τ decay [1,2,28,29,4], we calculate the QCD correction to the $R_{e^+e^-}$ ratio by using the contour integral representation [30,31] and evaluating the contour integral numerically. In this way we resum to all orders some of the so-called π^2 corrections, which appear as a result of analytic

continuation of the expression for the hadronic vacuum polarization function from spacelike to timelike momenta [32,33]. Such corrections constitute a dominant contribution in the NNLO. Using the improved expression we perform similar analysis as in the case of the conventional expansion. We find that the predictions obtained by numerical evaluation of the contour integral show extremely good stability with respect to change of the RS. The results reported here have been announced in [3] and briefly described in [5].

II. $\delta_{e^+e^-}$ AND THE PROBLEM OF RENORMALIZATION SCHEME AMBIGUITY

Away from the thresholds, neglecting the effects of the quark masses and the electroweak corrections, the formula for $R_{e^+e^-}$ may be written in the form

$$R_{e^+e^-}(s) = 3\sum_f Q_f^2[1 + \delta_{e^+e^-}(s)], \qquad (2)$$

where Q_f denotes the electric charge of the quark with the flavor f and $\delta_{e^+e^-}$ is the QCD correction. The renormalization group improved NNLO expression for $\delta_{e^+e^-}$ has the form

$$\delta_{e^+e^-}^{(2)}(s) = a(s)[1 + r_1 a(s) + r_2 a^2(s)], \qquad (3)$$

where $a(\mu^2) = g^2(\mu^2)/(4\pi^2)$ is the coupling constant, satisfying the renormalization group equation

$$\mu \frac{da}{d\mu} = -ba^2(1 + c_1 a + c_2 a^2). \qquad (4)$$

The perturbative result for $\delta_{e^+e^-}^{(2)}$ is usually expressed in the modified minimal subtraction ($\overline{\text{MS}}$) renormalization scheme, i.e., using the $\overline{\text{MS}}$ renormalization convention [34] with $\mu^2 = s$. In the $\overline{\text{MS}}$ scheme we have [35,7,8]

$$r_1^{\overline{\text{MS}}} = 1.985\,707 - 0.115\,295 n_f, \qquad (5)$$

TABLE I. Numerical values of the expansion coefficients r_i for $\delta_{e^+e^-}^{(2)}$, obtained with the $\overline{\text{MS}}$ renormalization convention and $\mu^2 = s$, for various numbers of quark flavors. The magnitude of the flavor singlet contribution r_2^{sing} is separately indicated. The values of the RS invariant ρ_2^R are calculated according to Eq. (9). The numerical values of the coefficients c_i in the renormalization group equation are included for completeness.

n_f	$r_1^{\overline{\text{MS}}}$	$r_2^{\overline{\text{MS}}}$	r_2^{sing}	c_1	$c_2^{\overline{\text{MS}}}$	ρ_2^R
2	1.75512	-9.14055	-0.08264	1.98276	5.77598	-9.92498
3	1.63982	-10.28394	0.00000	1.77778	4.47106	-11.41713
4	1.52453	-11.68560	-0.16527	1.54000	3.04764	-13.30991
5	1.40923	-12.80463	-0.03756	1.26087	1.47479	-15.09262
6	1.29394	-14.27207	-0.24791	0.92857	-0.29018	-17.43803

$$r_2^{\overline{\text{MS}}} = 18.242\,692 - 4.215\,847 n_f + 0.086\,207 n_f^2$$
$$+ r_2^{\text{sing}} - (b\pi/2)^2/3, \tag{6}$$

where the r_2^{sing} term in $r_2^{\overline{\text{MS}}}$ represents the so-called flavor singlet contribution,

$$r_2^{\text{sing}} = \frac{(\Sigma_f Q_f)^2}{\Sigma_f Q_f^2}\left(\frac{55}{216} - \frac{5}{9}\zeta_3\right), \tag{7}$$

which arises from the light-by-light scattering-type diagrams ($\zeta_3 = 1.202\,056\,903$). (It should be noted that the first calculation of the NNLO correction [6] was erroneous. The corrected result was published in [8]. An independent evaluation was reported in [7].) For the coefficients in the renormalization group equation we have $b = (33 - 2n_f)/6$, $c_1 = (153 - 19n_f)/(66 - 4n_f)$ and [36]

$$c_2^{\overline{\text{MS}}} = \frac{77\,139 - 15\,099 n_f + 325 n_f^2}{288(33 - 2n_f)}. \tag{8}$$

For convenience we collect in Table I the numerical values of the expansion coefficients for various values of n_f.

In addition to the $\overline{\text{MS}}$ scheme other choices of the RS are of course possible, such as for example the momentum subtraction schemes [37]. A change in the RS modifies the values of the expansion coefficients — the relevant formulas have been collected for example in [1]. (The coefficients b and c_1 are RS independent in the class of mass and gauge independent schemes.) The change in the expansion coefficients compensates for the finite renormalization of the coupling constant. Of course, in the given order of perturbation expansion this compensation may be only approximate, so that there is some numerical difference in the perturbative predictions in various schemes. This difference is formally of higher order in the coupling — it is $O(a^4)$ for the NNLO expression — but numerically the difference may be significant for comparison of theoretical predictions with the experimental data. There has been a lively discussion how to avoid this problem, both in the general case [38–41] (for a summary of early contributions see [42]) and in the particular case of $\delta_{e^+e^-}$ [11–20]. (Some of the early papers [11–15] contain a discussion of $\delta_{e^+e^-}^{(2)}$ with the erroneous value of the NNLO correction reported in [6]. Much of the initial

interest in the RS dependence of $\delta_{e^+e^-}^{(2)}$ came from the fact that this erroneous correction was very large.) It seems that one of the most interesting propositions is to choose the scheme according to the so-called principle of minimal sensitivity (PMS) [39].

However, as was emphasized in [1–3], in addition to calculating the predictions in some preferred renormalization scheme, it is also important to investigate the stability of the predictions with respect to reasonable variations in the scheme parameters. By calculating the variation in the predictions over some set of *a priori* acceptable schemes one obtains a quantitative estimate of reliability of the optimized predictions. A systematic method for analyzing the stability of predictions with respect to change of the renormalization scheme has been presented in [1–3]. This method is based on the existence of the RS-invariant combination of the expansion coefficients [38,39,41]:

$$\rho_2 = c_2 + r_2 - c_1 r_1 - r_1^2, \tag{9}$$

which appears to be a natural RS independent characterization of the magnitude of the NNLO correction. (We adopt here the definition of the RS invariant used in [38,41], which differs by a constant from the definition of Stevenson [39]: $\rho_2^{\text{Stev}} = \rho_2 - c_1^2/4$. The arguments in favor of Eq. (9) have been given in [3].) The numerical values of this invariant in the case of $\delta_{e^+e^-}$, for different values of n_f, are collected in Table I.

The ρ_2 invariant may be used to eliminate from the analysis the unnatural renormalization schemes. This is done by introducing a function σ_2 defined on the space of the expansion coefficients:

$$\sigma_2(r_1, r_2, c_2) = |c_2| + |r_2| + c_1|r_1| + r_1^2, \tag{10}$$

which measures the degree of cancellation in the expression for ρ_2. An unnatural renormalization scheme, which artificially introduces large expansion coefficients, would be immediately distinguished by a value of σ_2 which would be large compared to $|\rho_2|$. The function σ_2 defines classes of equivalence of the perturbative approximants. If one has any preference for using a perturbative expression obtained in some optimal scheme, one should also take into account predictions obtained in the schemes which imply the same, or smaller, cancellations in the expression for ρ_2, i.e., which have the same, or smaller, value of σ_2. In particular, for the PMS scheme we have $\sigma_2 \approx 2|\rho_2|$ [3]. Therefore it appears that the set of schemes which generate approximants satisfying $\sigma_2 \lesssim 2|\rho_2|$ is a minimal set that has to be taken into account in the analysis of stability of the predictions with respect to change of the RS. More generally, it is useful to use a condition on the allowed schemes in the form

$$\sigma_2(r_1, r_2, c_2) \lesssim l|\rho_2|, \tag{11}$$

where $l \geq 1$ is some constant, which determines how strong cancellations in the expression for ρ_2 we want to allow.

In this work we analyze the RS dependence of the NNLO predictions for $\delta_{e^+e^-}$, using systematically condition (11). As in previous papers [1–3], we use the r_1 and c_2 coefficients as the two independent parameters characterizing the freedom of choice of the approximants in the NNLO. To

obtain the numerical value of the running coupling constant we use the implicit equation, which results from integrating the renormalization group equation (4) with appropriate boundary condition [34]:

$$\frac{b}{2}\ln\left(\frac{s}{\Lambda_{\overline{MS}}^2}\right) = r_1^{\overline{MS}} - r_1 + \Phi(a, c_2),$$ (12)

where

$$\Phi(a, c_2) = c_1\ln\left(\frac{b}{2c_1}\right) + \frac{1}{a} + c_1\ln(c_1 a) + O(a).$$ (13)

The explicit form of $\Phi(a, c_2)$ is given for example in [43]. The appearance of $\Lambda_{\overline{MS}}$ and $r_1^{\overline{MS}}$ in expression (12) is a result of taking into account the so-called Celmaster-Gonsalves relation [37] between the lambda parameters in different schemes. This relation is valid to all orders of perturbation expansion.

The region of the scheme parameters satisfying Eq. (11) has a simple analytic description. In the case $\rho_2 < 0$ and $|\rho_2| > 2c_1^2(l+1)/(l-1)^2$ let us define

$$r_1^{min} = -\sqrt{|\rho_2|(l+1)/2},$$ (14)

$$r_1^{max} = [-c_1 + \sqrt{c_1^2 + 2(l+1)|\rho_2|}]/2,$$ (15)

$$c_2^{min} = -|\rho_2|(l+1)/2,$$ (16)

$$c_2^{max} = |\rho_2|(l-1)/2,$$ (17)

$$c_2^{int} = c_1 r_1^{min} + c_2^{max}.$$ (18)

For $c_2 > 0$ the region of allowed parameters is bounded from above by the line joining the points $(r_1^{min}, 0)$, (r_1^{min}, c_2^{int}), $(0, c_2^{max})$, (r_1^{max}, c_2^{max}), $(r_1^{max}, 0)$. For $c_2 < 0$ the region of allowed parameters is bounded from below by the lines

$$c_2(r_1) = r_1^2 + c_2^{min} \quad \text{for} \quad r_1^{min} \leq r_1 \leq 0,$$ (19)

$$c_2(r_1) = r_1^2 + c_1 r_1 + c_2^{min} \quad \text{for} \quad 0 \leq r_1 \leq r_1^{max}.$$ (20)

In the case $\rho_2 < 0$ and

$$|\rho_2| < 2c_1^2(l+1)/(l-1)^2$$ (21)

we should use instead

$$r_1^{min} = -|\rho_2|(l-1)/(2c_1),$$ (22)

$$c_2^{int} = (r_1^{min})^2 + c_2^{min}.$$ (23)

For $c_2 > 0$ the region of allowed parameters is then bounded from above by the line joining the points $(r_1^{min}, 0)$, $(0, c_2^{max})$, (r_1^{max}, c_2^{max}), $(r_1^{max}, 0)$. For $c_2 < 0$ the region of allowed parameters is bounded from below by the line joining the points $(r_1^{min}, 0)$ and (r_1^{min}, c_2^{int}), and the curves defined in the previous case.

For $\rho_2 > c_1^2/4$ the region of the scheme parameters satisfying Eq. (11) has been described in [3].
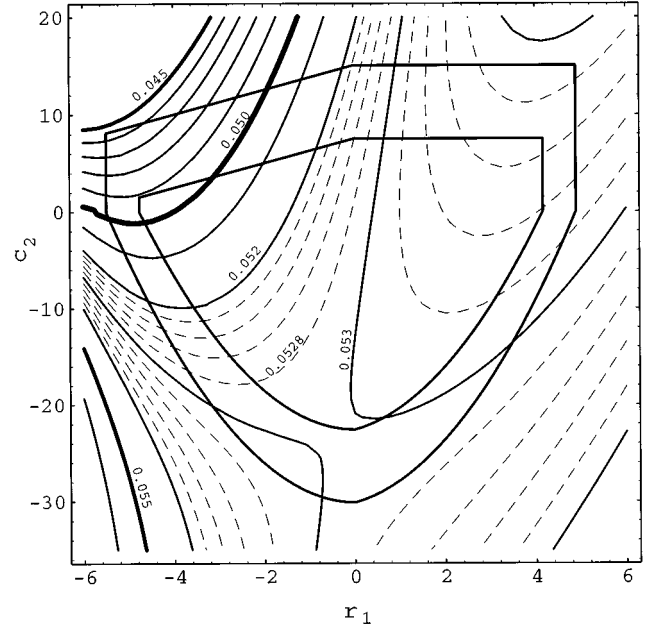

FIG. 1. The contour plot of $\delta_{e^+e^-}^{(2)}$ as a function of the parameters r_1 and c_2, with $n_f = 5$, for $\sqrt{s}/\Lambda_{\overline{MS}}^{(5)} = 75$. The region of scheme parameters satisfying condition (11) has been also indicated for $l = 2$ (the smaller region) and for $l = 3$.

III. ESTIMATE OF THE RS AMBIGUITIES IN THE CONVENTIONAL EXPANSION FOR $\delta_{e^+e^-}$

Let us first consider the case of five active quark flavors, which is most important for experimental determination of $\Lambda_{\overline{MS}}$. The same corrections give also a dominant QCD contribution to the hadronic width of the Z^0 boson. For $n_f = 5$ we have $\rho_2^R = -15.092\,62$. In Fig. 1 we show the contour plot of $\delta_{e^+e^-}^{(2)}$ as a function of the parameters r_1 and c_2, for $\sqrt{s}/\Lambda_{\overline{MS}}^{(5)} = 75$. We have indicated the region of parameters satisfying condition (11) with $l = 2$. For comparison, we also indicate the region corresponding to $l = 3$. The PMS prediction is represented in Fig. 1 by a saddle point at $r_1 = -0.408$ and $c_2 = -23.154$. We see that the PMS parameters are close to the approximate solution of the PMS equations [44]:

$$r_1^{PMS} = 0(a^{PMS}), \quad c_2^{PMS} = \frac{3}{2}\rho_2 + 0(a^{PMS}),$$ (24)

and the PMS point lies indeed on the boundary of the $l = 2$ region, as expected. Comparing the values of $\delta_{e^+e^-}^{(2)}$ obtained for the scheme parameters in the $l = 2$ region we find for $\sqrt{s}/\Lambda_{\overline{MS}}^{(5)} = 75$, that the minimal value is attained for $r_1 = -4.76$, $c_2 = 1.55$ and the maximal value is attained for $r_1 = 3.52$, $c_2 = 7.55$. For the $l = 3$ region we obtain the minimal value for $r_1 = -5.49$, $c_2 = 8.17$, and the maximal value for $r_1 = 3.98$, $c_2 = 15.09$. In both cases the maximal and minimal values are attained at the boundary of the allowed region. Let us note, that the commonly used $\overline{MS}$ scheme lies within the $l = 2$ region.

Performing similar contour plots in the range $40 < \sqrt{s}/\Lambda_{\overline{MS}}^{(5)} < 200$ we find that the scheme parameters, for
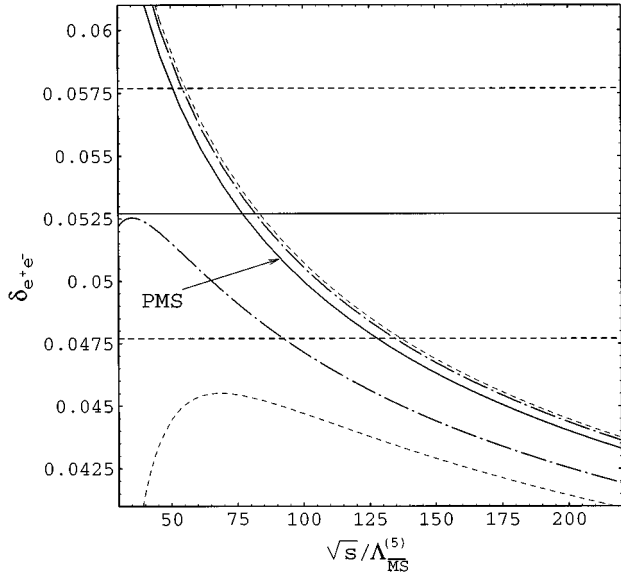
FIG. 2. The maximal and minimal values of $\delta^{(2)}_{e^+e^-}$ in the $l=2$ (dash-dotted line) and $l=3$ (dashed line) allowed regions, with $n_f=5$, as a function of $\sqrt{s}/\Lambda^{(5)}_{\overline{\text{MS}}}$. The PMS prediction is also shown, and the experimental constraint $\delta^{\text{expt}}_{e^+e^-}(\sqrt{s}=31.6 \text{ GeV})=0.0527\pm0.0050$ [45] is indicated for comparison.

FIG. 3. The contour plot of $\delta^{(2)}_{e^+e^-}$ as a function of the parameters r_1 and c_2, with $n_f=4$, for $\sqrt{s}/\Lambda^{(4)}_{\overline{\text{MS}}}=30$. The region of scheme parameters satisfying condition (11) with $l=2$ has been also indicated.

which $\delta^{(2)}_{e^+e^-}$ reaches extremal values in the $l=2,3$ allowed regions, are practically independent of the $\sqrt{s}/\Lambda^{(5)}_{\overline{\text{MS}}}$.

In Fig. 2 we show how the maximal and minimal values of $\delta^{(2)}_{e^+e^-}$ in the $l=2,3$ allowed regions depend on $\sqrt{s}/\Lambda^{(5)}_{\overline{\text{MS}}}$. We also show the PMS prediction and the experimental constraint $\delta^{\text{expt}}_{e^+e^-}(\sqrt{s}=31.6 \text{ GeV})=0.0527\pm0.0050$ [45]. We find that with increasing $\sqrt{s}/\Lambda^{(5)}_{\overline{\text{MS}}}$ the scheme dependence is decreasing, as expected, although it remains substantial even for high energies. Let us take for example $\sqrt{s}/\Lambda^{(5)}_{\overline{\text{MS}}}=162$, corresponding to $\Lambda^{(5)}_{\overline{\text{MS}}}=0.195$ GeV — which is the value preferred by the Particle Data Group [46] — and $\sqrt{s}=31.6$. In this case the scheme variation of $\delta^{(2)}_{e^+e^-}$ over the $l=2$ region is 5% of the PMS prediction, and for the $l=3$ region 8%, compared with 9% and 16%, respectively, for $\sqrt{s}/\Lambda^{(5)}_{\overline{\text{MS}}}=75$. However, when we decrease $\sqrt{s}/\Lambda^{(5)}_{\overline{\text{MS}}}$ below 75 the scheme dependence increases rapidly, and it becomes very large already for $\sqrt{s}/\Lambda^{(5)}_{\overline{\text{MS}}}=30$. The scheme dependence appears to be quite large in the range of values of $\delta^{(2)}_{e^+e^-}$ relevant for fitting the experimental data. For example, the line representing the minimal values on the $l=2$ region does not reach the central experimental value, which translates into a very large theoretical uncertainty in the fitted value of $\Lambda_{\overline{\text{MS}}}$.

For $n_f=4$ we have $\rho^R_2=-13.309\,91$. In Fig. 3 we show the contour plot of $\delta^{(2)}_{e^+e^-}$ as a function of the parameters r_1 and c_2, for $\sqrt{s}/\Lambda^{(4)}_{\overline{\text{MS}}}=30$. Similarly as in the $n_f=5$ case we find that the PMS prediction is well represented by the approximate solution (24). The variation over the $l=2$ region is approximately 11% of the PMS prediction. In Fig. 4 we show the variation in the predictions for $\delta^{(2)}_{e^+e^-}$ when the scheme parameters are changed over the $l=2$ region, as a
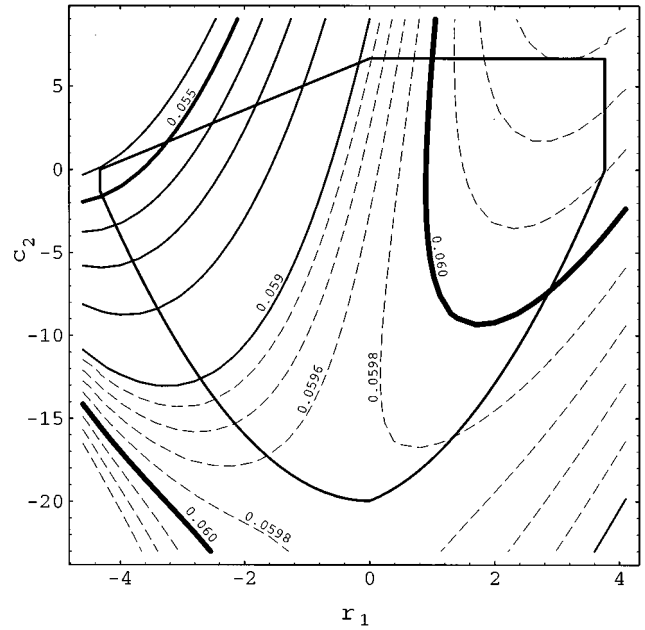
function of $\sqrt{s}/\Lambda^{(4)}_{\overline{\text{MS}}}$. It is evident that for $\sqrt{s}/\Lambda^{(4)}_{\overline{\text{MS}}}$ smaller than 20, which is the range relevant for fitting the experimental data, this variation becomes very large. (Note that analysis of experimental data from several experiments gives [45] $\delta^{\text{expt}}_{e^+e^-}(\sqrt{s}=9 \text{ GeV})=0.073\pm0.024$.)

Finally, for $n_f=3$ we have $\rho^R_2=-11.417\,13$. In Fig. 5 we
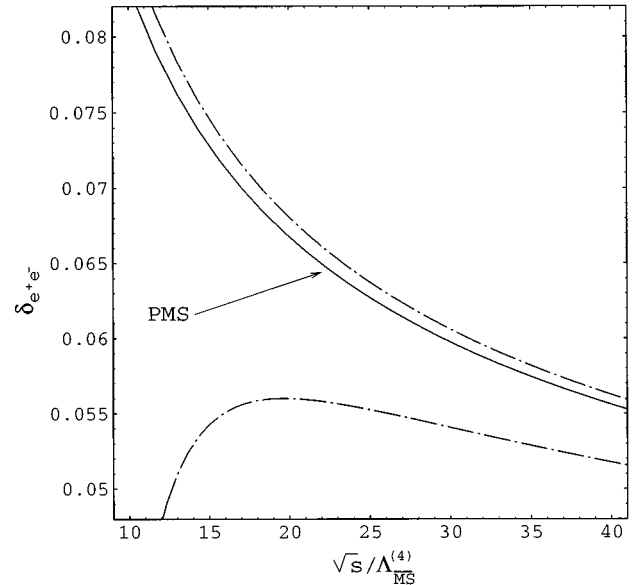

FIG. 4. The variation in the predictions for $\delta^{(2)}_{e^+e^-}$ when the scheme parameters are changed over the $l=2$ region, with $n_f=4$, as a function of $\sqrt{s}/\Lambda^{(4)}_{\overline{\text{MS}}}$. The upper curve corresponds to $r_1=3.10$ and $c_2=6.65$, the lower curve corresponds to $r_1=-4.32$ and $c_2=0$. For comparison the PMS prediction is shown.
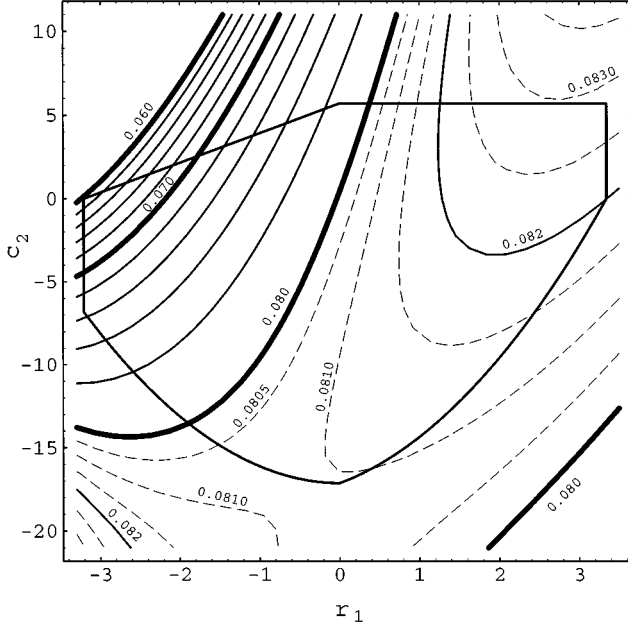
FIG. 5. Same as in Fig. 3 but for $n_f = 3$ and $\sqrt{s}/\Lambda_{\overline{\mathrm{MS}}}^{(3)} = 9$.

show the contour plot of $\delta_{e^+e^-}^{(2)}$ as a function of the parameters r_1 and c_2, for $\sqrt{s}/\Lambda_{\overline{\mathrm{MS}}}^{(3)} = 9$. The variation of the predictions over the $l = 2$ region is approximately 28% of the PMS value. In Fig. 6 we show the variation in the predictions for $\delta_{e^+e^-}^{(2)}$ when the scheme parameters are changed over the $l = 2$ region, as a function of $\sqrt{s}/\Lambda_{\overline{\mathrm{MS}}}^{(3)}$. We observe that the variation in the predictions starts to increase rapidly for $\sqrt{s}/\Lambda_{\overline{\mathrm{MS}}}^{(3)}$ smaller than 9.
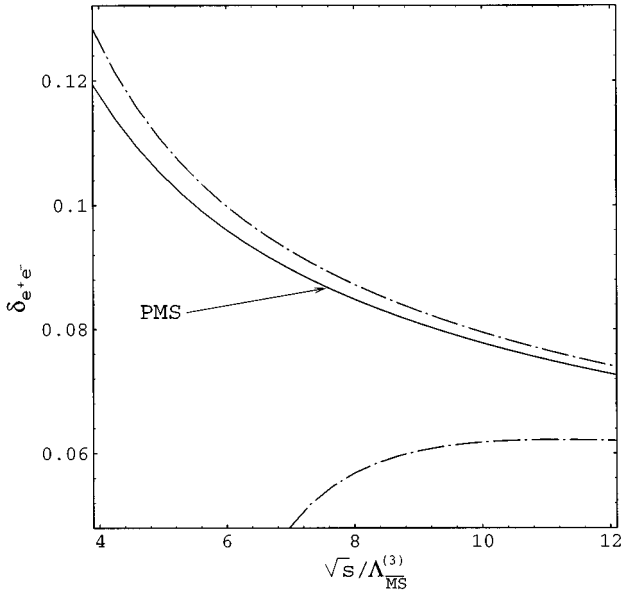

FIG. 6. The variation in the predictions for $\delta_{e^+e^-}^{(2)}$ when the scheme parameters are changed over the $l = 2$ region, with $n_f = 3$, as a function of $\sqrt{s}/\Lambda_{\overline{\mathrm{MS}}}^{(3)}$. The upper curve corresponds to $r_1 = 2.71$ and $c_2 = 5.71$, the lower curve corresponds to $r_1 = -3.21$ and $c_2 = 0$. For comparison the PMS curve is shown.

Let us summarize our analysis of the predictions for $\delta_{e^+e^-}$ obtained from the conventional expansion. We found that changing the renormalization scheme within a class of schemes which, according to our condition (11), appear to be as good as the PMS scheme, we obtain rather large variation in the predictions. In some cases we may even speak about instability of the predictions with respect to change of the renormalization scheme. This is in contrast with the statement in [16], that the conventional expansion for $\delta_{e^+e^-}$ is highly reliable. The conclusion found in [16] is based on the observation, that for $\delta_{e^+e^-}$ the $\overline{\mathrm{MS}}$ prediction is very close to the PMS prediction. The fact that the $\overline{\mathrm{MS}}$ prediction is very close to the PMS prediction is of course true — for example in the scale of Fig. 2 the $\overline{\mathrm{MS}}$ and PMS curves would be difficult to distinguish. Similar situation occurs for other values of n_f. It is clear however, that there is no theoretical or phenomenological motivation to use the $\overline{\mathrm{MS}}$-PMS difference as a measure of reliability of the perturbation expansion for any physical quantity. The fact that the $\overline{\mathrm{MS}}$ prediction for $\delta_{e^+e^-}$ is close to the PMS prediction is simply a coincidence, without deeper significance for such problems as reliability of the predictions and good or bad convergence of the perturbation expansion.

It is interesting to note that for very low energies the PMS predictions display the infrared fixed point type of behavior [18]. However, this type of behavior, which in fact does not manifest itself in the $n_f = 3$ predictions until $\sqrt{s}/\Lambda_{\overline{\mathrm{MS}}}^{(3)} \approx 2.5$, is accompanied by a rapidly increasing RS dependence. It seems therefore unreasonable to put too much faith in the PMS prediction when even a very small change of the scheme parameters dramatically modifies the result. These remarks apply as well to the case $n_f = 2$.

IV. ANALYSIS OF THE π^2 TERMS IN $\delta_{e^+e^-}$

The strong RS dependence described above is somewhat surprising. It may seem understandable that the perturbation expansion is not reliable in the energy range appropriate for example for the $n_f = 3$ regime. However, one would expect that $\sqrt{s}/\Lambda_{\overline{\mathrm{MS}}}^{(5)}$ of order 75 is large enough for the perturbation series to be very well behaved. The origin of the strong scheme dependence may be traced back to the fact that the NNLO correction is relatively large, which is reflected by large value of the RS invariant ρ_2^R. However, a major contribution to the NNLO correction comes from the term which appears in the process of analytic continuation of perturbative expression from spacelike to timelike momenta. To see clearly the significance of such contributions, and to show how one may treat them in an improved way, it is convenient to use the so-called Adler function [47],

$$D(q^2) = -12\pi^2 q^2 \frac{d}{dq^2} \Pi(q^2), \qquad (25)$$

where $\Pi(q^2)$ is the transverse part of quark electromagnetic current correlator $\Pi^{\mu\nu}(q)$:

$$\Pi^{\mu\nu}(q) = (-g^{\mu\nu}q^2 + q^\mu q^\nu)\Pi(q^2), \qquad (26)$$

$$\Pi^{\mu\nu}(q) = i \int d^4x \, e^{iqx} \langle 0|T[J^\mu(x)J^\nu(0)^\dagger]|0\rangle. \quad (27)$$

Neglecting the quark mass effects and electroweak corrections we may write

$$D(q^2) = 3 \sum_f Q_f^2 [1 + \delta_D(-q^2)], \quad (28)$$

where $\delta_D(-q^2)$ denotes the QCD correction. The Adler function is RS invariant in the formal sense; i.e., it may be considered to be a physical quantity, despite the fact that it cannot be directly measured in the experiment. In particular, $\delta_D(-q^2)$ is renormalization group invariant, in contrast to $\Pi(q^2)$, which does not even satisfy a homogenous renormalization group equation [48]. The Adler function is directly calculable in the perturbation expansion for spacelike momenta. To express the $R_{e^+e^-}$ ratio by the Adler function one inverts the relation (25):

$$\Pi(q^2) - \Pi(q_0^2) = -\frac{1}{12\pi^2} \int_{q_0^2}^{q^2} d\sigma \frac{D(\sigma)}{\sigma}, \quad (29)$$

where q_0^2 is some reference spacelike momentum, and one utilizes the relation:

$$R_{e^+e^-}(s) = 12\pi \, \mathrm{Im}\Pi(s+i\epsilon) = \frac{6\pi}{i}[\Pi(s+i\epsilon) - \Pi(s-i\epsilon)]. \quad (30)$$

In this way one obtains $R_{e^+e^-}(s)$ as a contour integral in the complex momentum plane, with the Adler function under the integral [30,31]:

$$R_{e^+e^-}(s) = -\frac{1}{2\pi i} \int_C d\sigma \frac{D(\sigma)}{\sigma}, \quad (31)$$

where the contour C runs clockwise from $\sigma = s - i\epsilon$ to $\sigma = 0$ below the real positive axis, around $\sigma = 0$, and to $\sigma = s + i\epsilon$ above the real positive axis. The integration contour may be of course arbitrarily deformed in the domain of

TABLE II. Numerical values of the RS-invariant ρ_2^D characteristic for the QCD correction to the Adler function.

n_f	ρ_2^D
2	9.28877
3	5.23783
4	0.96903
5	-3.00693
6	-7.36281

analyticity of the Adler function. A convenient choice is $q^2 = -s \exp(-i\theta)$ with $\theta \in [-\pi, \pi]$. For this choice of the contour we obtain the following simple relation between $\delta_{e^+e^-}(s)$ and $\delta_D(-q^2)$:

$$\delta_{e^+e^-}(s) = \frac{1}{2\pi} \int_{-\pi}^{\pi} d\theta [\delta_D(-\sigma)|_{\sigma = -s\exp(-i\theta)}], \quad (32)$$

The conventional expression for $\delta_{e^+e^-}(s)$ may be recovered from this formula by inserting under the contour integral an expansion of $\delta_D(-q^2)$ in terms of $a(s)$:

$$\begin{aligned}\delta_D^{(2)}(-q^2) = a(s)(1 + [\hat{r}_1 - (b/2)\ln(-q^2/s)]a(s) \\ + \{\hat{r}_2 - (c_1 + 2\hat{r}_1)(b/2)\ln(-q^2/s) \\ + (b/2)^2[\ln(-q^2/s)]^2\}a^2(s)), \quad (33)\end{aligned}$$

where $\hat{r}_i$ denote the coefficients for expansion of $\delta_D(-q^2)$ in terms of $a(-q^2)$. Evaluating the trivial contour integrals involving powers of $\ln(-\sigma/s)$, we obtain expression (3) with

$$r_1 = \hat{r}_1, \quad r_2 = \hat{r}_2 - \frac{1}{3}\left(\frac{b\pi}{2}\right)^2. \quad (34)$$

This implies $\rho_2^R = \rho_2^D - (b\pi/2)^2/3$. In Table II we list the values of ρ_2^D for various values of n_f.

Numerically the contribution of the π^2 term is very large — for example for $n_f = 5$ we have $\rho_2^R - \rho_2^D = -12.085\,70$.

Contributions proportional to π^2 appear also in higher orders. We have [25]

$$r_3 = \hat{r}_3 - \left(\hat{r}_1 + \frac{5}{6}c_1\right)\left(\frac{b\pi}{2}\right)^2, \quad (35)$$

$$r_4 = \hat{r}_4 - \left(2\hat{r}_2 + \frac{7}{3}c_1\hat{r}_1 + \frac{1}{2}c_1^2 + c_2\right)\left(\frac{b\pi}{2}\right)^2 + \frac{1}{5}\left(\frac{b\pi}{2}\right)^4. \quad (36)$$

The result for r_5 may be found in [22]

$$r_5 = \hat{r}_5 - \frac{1}{3}\left(10\hat{r}_3 + \frac{27}{2}c_1\hat{r}_2 + 4c_1^2\hat{r}_1 + \frac{7}{2}c_1c_2 + 8c_2\hat{r}_1 + \frac{7}{2}c_3\right)\left(\frac{b\pi}{2}\right)^2 + \frac{1}{5}\left(5\hat{r}_1 + \frac{77}{12}c_1\right)\left(\frac{b\pi}{2}\right)^4. \quad (37)$$

(The difference between r_i and $\hat{r}_i$ in higher orders was studied in [25,26,33].) Note that the π^2 corrections to $\hat{r}_3$ and $\hat{r}_4$ are fully determined by the NNLO expression for $\delta_D(-q^2)$. Taking into account that we have the following expressions for the higher-order RS-invariant combinations of the expansion coefficients [41]:

$$\rho_3 = c_3 + 2r_3 - 4r_2r_1 - 2r_1\rho_2 - r_1^2 c_1 + 2r_1^3, \qquad (38)$$

$$\rho_4 = c_4 + 3r_4 - 6r_3r_1 - 4r_2^2 - 3r_1\rho_3 - 4r_1^4 - (r_2 + 2r_1^2)\rho_2$$
$$+ 11r_2r_1^2 + c_1(r_3 - 3r_2r_1 + r_1^3). \qquad (39)$$

We obtain

$$\rho_3^R = \rho_3^D - \frac{5}{3}c_1\left(\frac{b\pi}{2}\right)^2, \qquad (40)$$

$$\rho_4^R = \rho_4^D - \frac{1}{3}(8\rho_2^D + 7c_1^2)\left(\frac{b\pi}{2}\right)^2 + \frac{2}{45}\left(\frac{b\pi}{2}\right)^4. \qquad (41)$$

The π^2 terms are quite sizable numerically. For example for $n_f = 5$ we have

$$\rho_3^R - \rho_3^D = -76.1924, \quad \rho_4^R - \rho_4^D = 211.025. \qquad (42)$$

It is evident that the terms arising from the analytic continuation would make a significant contribution to the RS invariants in any order of the perturbation expansion.

Returning to the evaluation of $\delta_{e^+e^-}(s)$, we note that the procedure used to obtain the conventional result treats the q^2 dependence of δ_D in the complex energy plane in a rather crude way. A straightforward way to improve this evaluation is to use under the contour integral the renormalization group improved expression for $\delta_D(-\sigma)$, analytically continued from the real negative σ to the whole complex energy plane cut along the real positive axis. In other words, one should take into account the renormalization group evolution of $a(-\sigma)$ in the complex energy plane, avoiding the expansion of $a(-\sigma)$ in terms of $a(s)$. In this way one makes maximal use of the renormalization group invariance property of the Adler function. Of course the integral may be now done only numerically, and the resulting expression for $\delta_{e^+e^-}(s)$ is no longer a polynomial in $a(s)$, despite the fact that only the NNLO expression for the Adler function is used. It is easy to convince onself that the procedure outlined above is equivalent to the resummation — to all orders — of the π^2 terms that contain powers of b, c_1, and/or c_2. (The summation of the leading terms proportional to $(b\pi/2)^2$ was discussed in [33].)

The improved approach based on the contour integral has been implemented with success in the case of the QCD corrections to the τ lepton decay [28,29,4], where a similar problem of strong renormalization scheme dependence appears. It was found that using the contour integral representation and evaluating the contour integral numerically one obtains considerable improvement in the stability of predictions with respect to change of RS [29,4]. It is therefore of great interest to see whether one may improve in this way the predictions for $\delta_{e^+e^-}$.
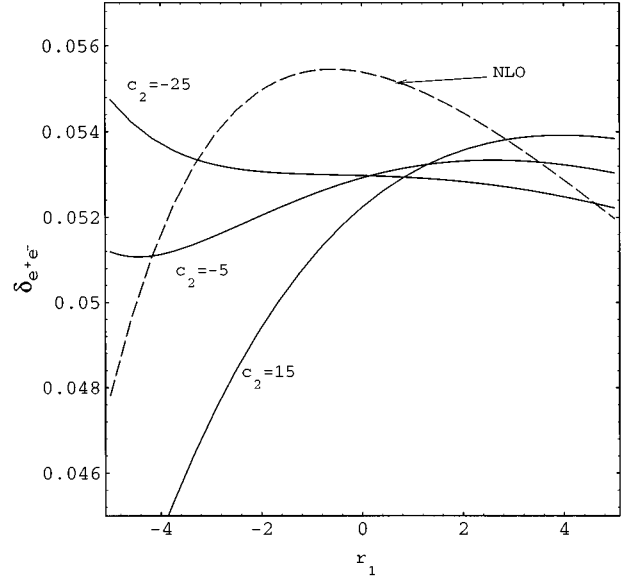

FIG. 7. $\delta_{e^+e^-}^{(2)}$ as a function of r_1, for several values of c_2, for $n_f = 5$ and $\sqrt{s}/\Lambda_{\overline{\mathrm{MS}}}^{(5)} = 75$, obtained with the conventional NNLO expression. For comparison also the NLO predictions are indicated.

V. IMPROVED EVALUATION OF $\delta_{e^+e^-}$

In this section we perform an analysis similar to that in Sec. III, using now the improved predictions for $\delta_{e^+e^-}$, obtained by evaluating numerically the contour integral in Eq. (32). Similarly as in the case of the conventional perturbation expansion, we begin with the $n_f = 5$ case. To show, how the improved evaluation of $\delta_{e^+e^-}^{(2)}$ affects its RS dependence, we compare the plots of $\delta_{e^+e^-}^{(2)}$ as a function of r_1, for several values of c_2, with $\sqrt{s}/\Lambda_{\overline{\mathrm{MS}}}^{(5)} = 75$, obtained with the conventional NNLO expression (Fig. 7) and with the numerical evaluation of the contour integral (Fig. 8). We see that the predictions obtained by the numerical evaluation of the contour integral have much smaller RS dependence. In Fig. 8 we have also indicated the predictions obtained with the conventional expansion supplemented by the $O(a^4)$ and $O(a^5)$ terms given by Eq. (35) and Eq. (36). We see that this type of simple improvement of the conventional expansion reproduces quite well the results obtained from exact contour integral, except for large negative r_1. [Inclusion of only the $O(a^4)$ term does not give good approximation. Inclusion of the $O(a^6)$ correction given by Eq. (37), which is of course only partially known at present, slightly improves the approximation for positive r_1.]

In Fig. 9 we show the contour plot of $\delta_{e^+e^-}^{(2)}$ obtained from the expression (32) for $\sqrt{s}/\Lambda_{\overline{\mathrm{MS}}}^{(5)} = 75$. In Fig. 9 we also show the relevant regions of the scheme parameters satisfying condition (11) with $l = 2,3$. These regions are calculated assuming $\rho_2 = \rho_2^D$, because the basic object in the improved approach is $\delta_D^{(2)}$. For $n_f = 5$ we have $\rho_2^D = -3.006\,93$, which is much smaller in absolute value than ρ^R. Consequently, the region of the allowed scheme parameters is much smaller than in the analysis of the conventional NNLO approximant. The improved predictions for $\delta_{e^+e^-}$ have a saddle point type of behavior as a function of r_1 and c_2, where the saddle
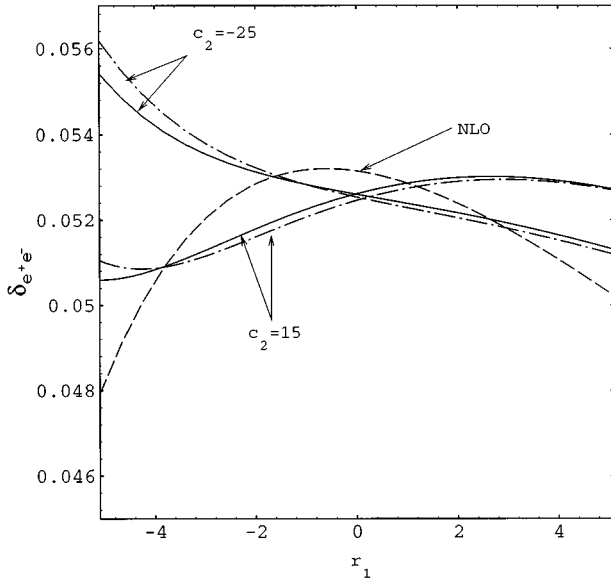
FIG. 8. $\delta_{e^+e^-}^{(2)}$ as a function of r_1, for several values of c_2, for $n_f=5$ and $\sqrt{s}/\Lambda_{\overline{MS}}^{(5)}=75$, obtained with the numerical evaluation of the contour integral. For comparison also the NLO predictions are indicated, and the predictions obtained from the conventional expansion supplemented by the $O(a^4)$ and $O(a^5)$ corrections given by Eq. (35) and Eq. (36).

point represents the PMS prediction. However, the location of the saddle point is completely different than in the case of conventional expansion. (The location of the saddle point for the improved expression is no longer a solution of the set of the PMS equations given in [39], because the improved approximant (32) is not a polynomial in the running coupling
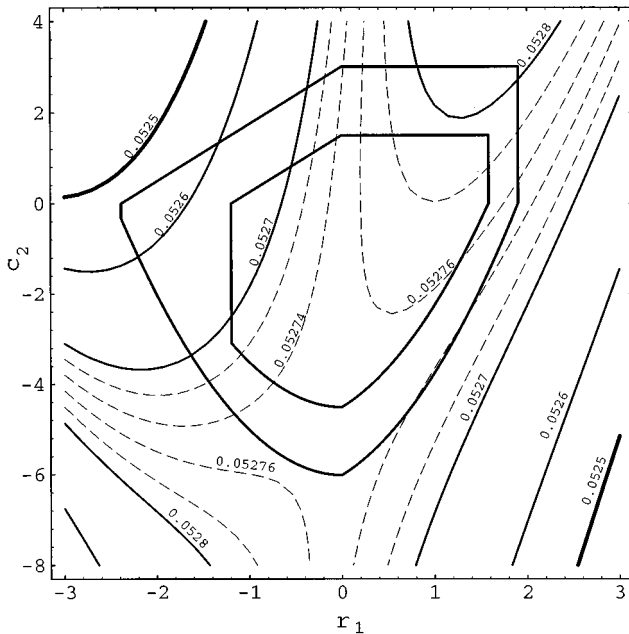

FIG. 9. Contour plot of $\delta_{e^+e^-}^{(2)}$ obtained from the improved expression for $n_f=5$ and $\sqrt{s}/\Lambda_{\overline{MS}}^{(5)}=75$. The regions of scheme parameters satisfying condition (11) with $l=2$ (the smaller region) and $l=3$ have been indicated, assuming $\rho_2=\rho_2^D$.

TABLE III. Numerical values of the optimized predictions for $\delta_{e^+e^-}$, obtained from the contour integral expression (32) for $n_f=5$. The PMS parameters are well approximated by $r_1=0$, $c_2=1.5\rho_2^D$ (NNLO) and $r_1=-0.59$ (NLO).

$\sqrt{s}/\Lambda_{\overline{MS}}^{(5)}$	$\delta_{e^+e^-}^{opt,NNLO}$	$\delta_{e^+e^-}^{opt,NLO}$
25	0.06799	0.06888
50	0.05753	0.05811
75	0.05275	0.05320
100	0.04981	0.05019
200	0.04389	0.04415
500	0.03791	0.03809

constant.) It is interesting that the PMS point for the improved expression lies very close to the point $r_1=0$ and $c_2=1.5\rho_2^D=-4.51$, which corresponds to the approximate value of the PMS parameters if $\delta_D^{(2)}$ is optimized for spacelike momenta. Let us note that the $\overline{MS}$ scheme lies outside the $l=2$ region in this case. However, the $\overline{MS}$ prediction in the improved approach is very close to the improved PMS prediction: we have 0.052 79 and 0.052 75, respectively.

The variation of the predictions over the $l=2$ region is 0.3% of the PMS prediction, and variation over the $l=3$ region is 0.5% of the PMS prediction. Even if we take variation over the region corresponding to $l=10$ we obtain only 2.5% change in the predictions. We see that the improved prediction for $\delta_{e^+e^-}$ shows wonderful stability with respect to change of the RS. From Fig. 7 and Fig. 8 it is also clear that the difference between NNLO and NLO PMS predictions is much smaller in the case of the improved prediction — 0.9% of the NNLO result for $\sqrt{s}/\Lambda_{\overline{MS}}^{(5)}=75$ — than in the case of the conventional expansion — 4.7% of the NNLO result. We conclude, therefore, that the theoretical ambiguities involved in the evaluation of $\delta_{e^+e^-}^{(2)}$ are in fact very small, provided that the analytic continuation effects are treated with appropriate care. For completeness, we give in Table III the NNLO and NLO PMS predictions in the improved approach for several values of $\sqrt{s}/\Lambda_{\overline{MS}}^{(5)}$.

In the case of $n_f=5$ predictions it is interesting how the improved evaluation affects the fit to experimental data. Using the experimental constraint $\delta_{e^+e^-}^{expt}(\sqrt{s}=31.6$ GeV$)=0.0527\pm0.0050$ [45] and the improved PMS prediction we find $\Lambda_{\overline{MS}}^{(5)}=0.419\pm0.194$ GeV, which is equivalent in the three-loop approximation to $\alpha_s^{\overline{MS}}(M_Z^2)=0.1319\pm0.0100$. For comparison, using the conventional expansion in the $\overline{MS}$ scheme we obtain the central value of $\Lambda_{\overline{MS}}^{(5)}=0.399$ GeV $[\alpha_s^{\overline{MS}}(M_Z^2)=0.1308]$, while with the PMS prescription in the conventional expansion we get $\Lambda_{\overline{MS}}^{(5)}=0.410$ GeV $[\alpha_s^{\overline{MS}}(M_Z^2)=0.1314]$. We see therefore that improvement in the evaluation of $\delta_{e^+e^-}^{(2)}$ has small effect on the fitted values of the $\Lambda_{\overline{MS}}^{(5)}$ parameter.

For $n_f=4$ we have $\rho_2^D=0.969\,03$, i.e., the effect of π^2 corrections is even larger than in the $n_f=5$ case. The $n_f=4$ case is in all respects similar to the $n_f=5$ case, except for the fact that the reduction in RS dependence seems to be even stronger. In Fig. 10 and Fig. 11 we compare the plots of
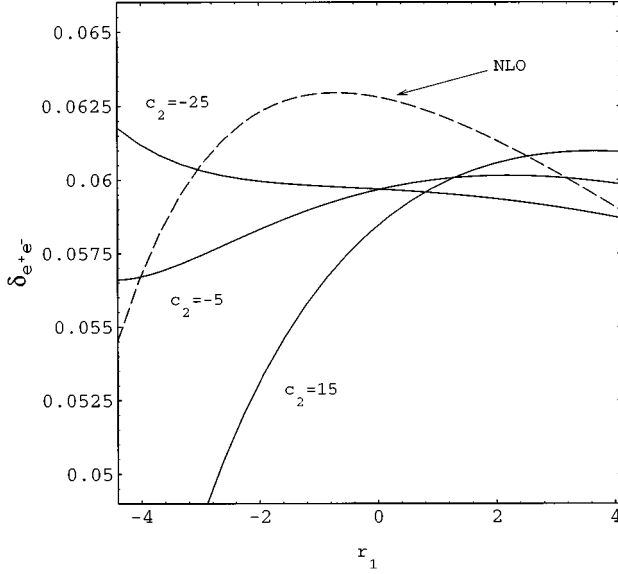
FIG. 10. Same as in Fig. 7, but for $n_f=4$ and $\sqrt{s}/\Lambda_{\overline{\rm MS}}^{(4)}=30$.

FIG. 12. Same as in Fig. 9, but for $n_f=4$ and $\sqrt{s}/\Lambda_{\overline{\rm MS}}^{(4)}=30$. Only the $l=2$ region has been indicated.

$\delta_{e^+e^-}^{(2)}$ as a function of r_1, for several values of c_2, with $\sqrt{s}/\Lambda_{\overline{\rm MS}}^{(4)}=30$, obtained with the conventional NNLO expression (Fig. 10) and with the numerical evaluation of the contour integral (Fig. 11). In Fig. 11 we also show the predictions obtained with the conventional expansion supplemented by the $O(a^4)$ and $O(a^5)$ terms given by Eq. (35) and Eq. (36). [Inclusion of the $O(a^6)$ correction (37) does not improve the approximation.] In Fig. 12 we show the contour plot of the improved prediction for $\delta_{e^+e^-}$ obtained for $\sqrt{s}/\Lambda_{\overline{\rm MS}}^{(4)}=30$. It is interesting that variation of the predictions over the $l=2$ region is extremely small, of the order of 0.03% of the PMS prediction. The improved prediction for $\sqrt{s}/\Lambda_{\overline{\rm MS}}^{(4)}=30$ in the $\overline{\rm MS}$ scheme is 0.059 02, quite close to the improved PMS result 0.059 07. The differences with the results obtained in the conventional approach again are not very big — using the conventional expansion we have
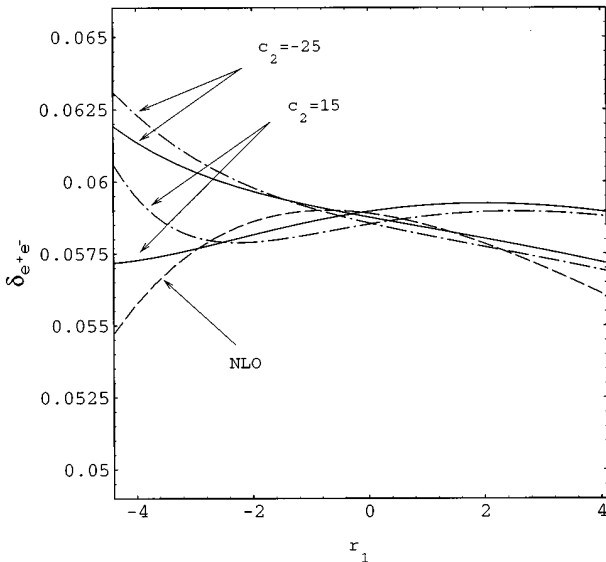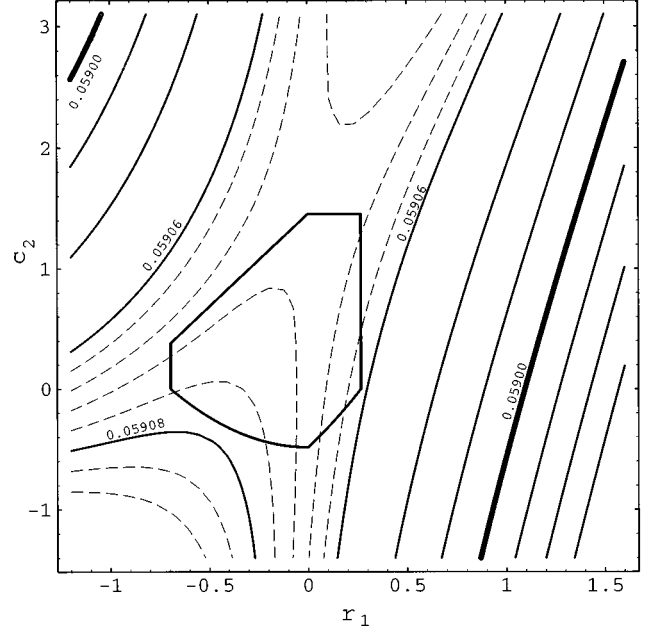
0.060 25 in the $\overline{\rm MS}$ scheme and 0.059 75 in the NNLO PMS. In Table IV we give numerical values of the improved predictions in the PMS scheme, for several values of $\sqrt{s}/\Lambda_{\overline{\rm MS}}^{(4)}$. We find that in the improved approach the NNLO PMS predictions are very close to NLO PMS predictions. We see therefore that also for $n_f=4$ the theoretical uncertainties in the improved predictions for $\delta_{e^+e^-}$ are very small.

Finally let us consider the case of $n_f=3$. We have then $\rho_2^D=5.237\,83$. In Fig. 13 and Fig. 14 we compare the plots of $\delta_{e^+e^-}^{(2)}$ as a function of r_1, for several values of c_2, with $\sqrt{s}/\Lambda_{\overline{\rm MS}}^{(3)}=9$, obtained with the conventional NNLO expression (Fig.13) and with the numerical evaluation of the contour integral (Fig. 14). Again, we find dramatic reduction in the RS dependence, despite rather low energy. It is interesting that in the $n_f=3$ case the addition of π^2 corrections given by Eq. (35) and Eq. (36) does not result in the improvement of the conventional predictions. In Fig. 15 we show the contour plot of $\delta_{e^+e^-}^{(2)}$ obtained from the improved expression for $\sqrt{s}/\Lambda_{\overline{\rm MS}}^{(3)}=9$. Similarly as for other numbers of flavors we obtain in the improved approach a very small variation in the predictions when parameters are changed

FIG. 11. Same as in Fig. 8, but for $n_f=4$ and $\sqrt{s}/\Lambda_{\overline{\rm MS}}^{(4)}=30$.

TABLE IV. Same as in Table II, but for $n_f=4$. The PMS parameter in NLO is approximately $r_1=-0.71$.

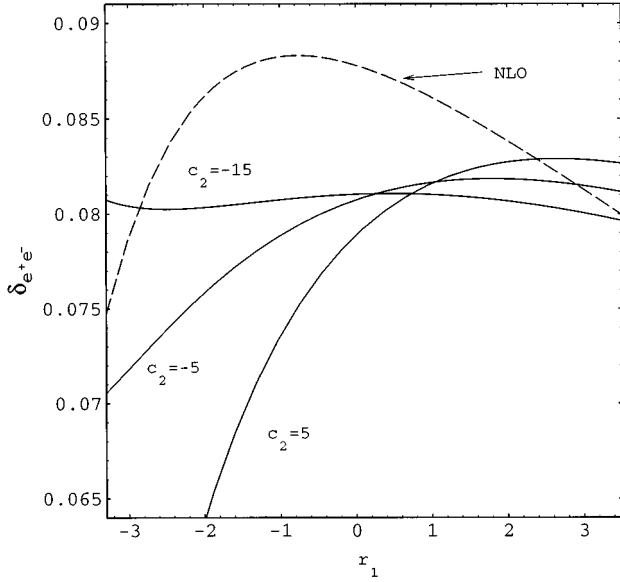| $\sqrt{s}/\Lambda_{\overline{\rm MS}}^{(4)}$	$\delta_{e^+e^-}^{\rm opt,\ NNLO}$	$\delta_{e^+e^-}^{\rm opt,\ NLO}$
10	0.08108	0.08093
20	0.06574	0.06565
30	0.05907	0.05900
40	0.05508	0.05503
50	0.05233	0.05228

FIG. 13. Same as in Fig. 7, but for $n_f = 3$ and $\sqrt{s}/\Lambda_{\overline{\text{MS}}}^{(3)} = 9$.

over the $l = 2$ region of parameters appropriate for $\delta_D^{(2)}$ — the variation is of the order of 0.8% of the PMS prediction 0.077 56. (We have verified that this situation persists down to $\sqrt{s}/\Lambda_{\overline{\text{MS}}}^{(3)} = 4$.) The improved prediction in the $\overline{\text{MS}}$ scheme is 0.077 19. For comparison, in the conventional approach we obtain 0.080 97 in the NNLO PMS and 0.082 44 in the NNLO $\overline{\text{MS}}$ scheme. In Table V we give numerical values of the improved predictions in the PMS scheme, for several values of $\sqrt{s}/\Lambda_{\overline{\text{MS}}}^{(3)}$. With this result we conclude, that the $n_f = 3$ NNLO expression for $\delta_{e^+e^-}$, obtained by evaluating the contour integral (32) numerically, has very small theoretical uncertainty, even for rather small values of $\sqrt{s}/\Lambda_{\overline{\text{MS}}}^{(3)}$. This situation is similar to that found for the QCD corrections to the τ decay [29,4].

The behavior of $\delta_{e^+e^-}^{(2)}$ at very low energies and the prob-
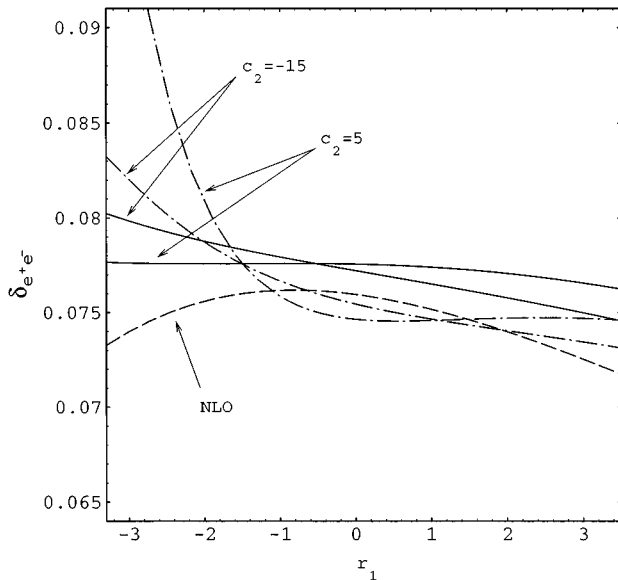

FIG. 14. Same as in Fig. 8, but for $n_f = 3$ and $\sqrt{s}/\Lambda_{\overline{\text{MS}}}^{(3)} = 9$.
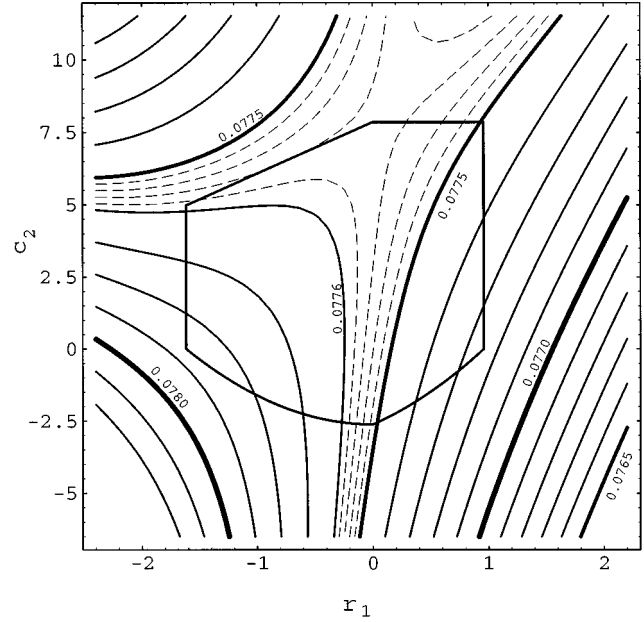

FIG. 15. Same as in Fig. 9, but for $n_f = 3$ and $\sqrt{s}/\Lambda_{\overline{\text{MS}}}^{(3)} = 9$. Only the $l = 2$ region has been indicated.

lem of existence of the fixed point in the improved approach would be discussed in a separate work [49].

VI. SUMMARY AND CONCLUSIONS

Summarizing, we have analyzed the RS dependence of the conventional NNLO expression for $\delta_{e^+e^-}$ using a systematic method described in [1–3]. We found rather large variation in the predictions. We have also investigated an improved way of calculating $\delta_{e^+e^-}^{(2)}$, which relies on a contour integral representation for this quantity and a numerical evaluation of the contour integral. We found that the stability of $\delta_{e^+e^-}^{(2)}$ with respect to change of the RS is greatly improved when the contour integral approach is used. Also, in the improved approach the difference between optimized NNLO and NLO predictions was found to be much smaller than in the case of the conventional expansion. We conclude therefore that the theoretical uncertainties in the NNLO QCD predictions for $\delta_{e^+e^-}$ are very small, even at low energies, provided that large π^2 terms, arising from analytic continuation, are treated with due care. We observed that the optimized predictions for $\delta_{e^+e^-}$, obtained in the contour integral approach, lie in general below the predictions from the opti-

TABLE V. Same as in Table II, but for $n_f = 3$. The PMS parameter in NLO is approximately $r_1 = -0.81$.

$\sqrt{s}/\Lambda_{\overline{\text{MS}}}^{(3)}$	$\delta_{e^+e^-}^{\text{opt, NNLO}}$	$\delta_{e^+e^-}^{\text{opt, NLO}}$
5	0.09624	0.09421
7	0.08475	0.08312
9	0.07756	0.07619
11	0.07255	0.07136
13	0.06879	0.06774

mized conventional expansion. However, for $n_f = 5$ the change in the fit of $\Lambda_{\overline{\rm MS}}^{(5)}$ to the experimental result came out to be small.

Note added. After this paper was completed, a related work was brought to our attention [50], in which the RS dependence of the QCD corrections to the total hadronic width of the Z boson is discussed. In [50] it is observed, that by using the contour integral to resum the large π^2 contributions one reduces the scale dependence of the QCD predictions. This result is in agreement with our observations, since the dominant contribution to $\Gamma_Z^{\rm had}$ comes from expression identical to $\delta_{e^+e^-}$. Let us note that the result reported in [50] was anticipated already in [3]. However, the approach adopted in [50] differs from our approach in several ways.

The authors of [50] do not discuss the choice of the range of scheme parameters used in their analysis. In their investigation of the conventional expansion for $\Gamma_Z^{\rm had}$ they use a smaller range of parameters than the one used above for $n_f = 5$. In particular, the PMS parameters are outside the range considered in [50]. In the analysis of improved predictions for $\Gamma_Z^{\rm had}$ the authors of [50] limit themselves to the discussion of the renormalization scale dependence, fixing the β function to the $\overline{\rm MS}$ value. There is also a technical difference that authors of [50] use approximate analytic expression for the running coupling constant to integrate along the contour in the complex energy plane, whereas we use exact numerical solution of the two- or three-loop renormalization group equation.

[1] P. A. Rączka, Phys. Rev. D **46**, R3699 (1992).

[2] P. A. Rączka, in *Proceedings of the XV International Warsaw Meeting on Elementary Particle Physics*, Kazimierz, Poland, 1992, edited by Z. Ajduk, S. Pokorski, and A. K. Wróblewski (World Scientific, Singapore, 1993), p. 496.

[3] P. A. Rączka, Z. Phys. C **65**, 481 (1995).

[4] P. A. Rączka and A. Szymacha, Z. Phys. C **70**, 125 (1996).

[5] P. A. Rączka, in *Proceedings of the XXXth Reucoutres de Morioud Conference '''95 QCD and High Energy Hadronic Interactions,''* Les Arcs, Savoie, France, 1995, edited by J. Trâu Thauh Vâu (Editious Frontieres, Gif-sur-Yvette, 1995), p. 279.

[6] S. G. Gorishny, A. L. Kataev, and S. A. Larin, Phys. Lett. B **212**, 238 (1988).

[7] L. R. Surguladze and M. A. Samuel, Phys. Rev. Lett. **66**, 560 (1991); **66**, 2416(E) (1991).

[8] S. G. Gorishny, A. L. Kataev, and S. A. Larin, Phys. Lett. B **259**, 144 (1991).

[9] D. J. Broadhurst and A. L. Kataev, Phys. Lett. B **315**, 179 (1993).

[10] K. G. Chetyrkin and J. H. Kühn, Nucl. Phys. **B432**, 337 (1994); Phys. Lett. B **342**, 356 (1995).

[11] C. J. Maxwell and J. A. Nicholls, Phys. Lett. B **213**, 217 (1988).

[12] A. P. Contogouris and N. Mebarki, Phys. Rev. D **39**, 1464 (1989).

[13] M. Haruyama, Prog. Theor. Phys. **82**, 380 (1989).

[14] P. A. Rączka and R. Rączka, Phys. Rev. D **40**, 878 (1989); Nuovo Cimento **104A**, 771 (1991).

[15] A. Dhar and V. Gupta, in *Proceedings of Workshop on Gauge Theories of Fundamental Interactions*, edited by M. Pawłowski and R. Rączka (World Scientific, Singapore, 1990).

[16] J. Chýla, A. Kataev, and S. A. Larin, Phys. Lett. B **267**, 269 (1991).

[17] M. Haruyama, Phys. Rev. D **45**, 930 (1992).

[18] A. C. Mattingly and P. M. Stevenson, Phys. Rev. Lett. **69**, 1320 (1992); Phys. Rev. D **49**, 437 (1994).

[19] H. J. Lu and S. J. Brodsky, Phys. Rev. D **48**, 3310 (1993); S. J. Brodsky and H. J. Lu, *ibid.* **51**, 3652 (1995); *Proceedings of the Tennessee International Symposium Radiative Corrections: Status and Outlook*, 1994, Gatlinburg, Tennessee, edited by B. F. L. Ward (World Scientific, Singapore, 1995), p. 451.

[20] L. R. Surguladze and M. A. Samuel, Phys. Lett. B**309**, 157 (1993).

[21] A. L. Kataev and V. V. Starshenko, in *QCD 94*, Proceedings of the International Workshop, Montpellier, France, 1994, edited by S. Narison [Nucl. Phys. B (Proc. Suppl.) **39BC**, 312 (1995)].

[22] A. L. Kataev and V. V. Starshenko, Mod. Phys. Lett. A **10**, 235 (1995).

[23] G. B. West, Phys. Rev. Lett. **67**, 1388 (1991); **67**, 3732(E) (1991); D. T. Barclay and C. J. Maxwell, *ibid.* **69**, 3417 (1992); J. Chýla, J. Fischer, and P. Kolář, Phys. Rev. D **47**, 2578 (1993); A. H. Duncan *et al.*, Phys. Rev. Lett. **70**, 4159 (1993).

[24] C. N. Lovett-Turner and C. J. Maxwell, Nucl. Phys. **B432**, 147 (1994); **B452**, 188 (1995).

[25] J. D. Bjorken, in *Particle Physics*, Proceedings of the Cargese Summer Institute in Particle Physics, Cargese, France, 1989, edited by M. Levy *et al.*, NATO Advanced Study Institute Series B: Physics Vol. 223 (Plenum, New York, 1990).

[26] L. S. Brown and L. G. Yaffe, Phys. Rev. D **45**, R398 (1992); L. S. Brown, L. G. Yaffe, and Chengxing Zhai, *ibid.* **46**, 4712 (1992).

[27] H. F. Jones and I. L. Solovtsov, Phys. Lett. B **349**, 519 (1995).

[28] A. A. Pivovarov, Z. Phys. C **53**, 461 (1992).

[29] F. LeDiberder and A. Pich, Phys. Lett. B **286**, 147 (1992).

[30] A. V. Radyushkin, Institution Report No. JINR E2-82-159, 1982 (unpublished).

[31] A. V. Radyushkin, *Proceedings of 9th CERN-JINR School of Physics*, 1985, Urbino, Italy [CERN Yellow Report No. CERN-86-03 (unpublished)], Vol. 1, p. 35.

[32] R. G. Moorhouse, M. R. Pennington, and G. G. Ross, Nucl. Phys. **B124**, 285 (1977); M. R. Pennington and G. G. Ross, Phys. Lett. **102B**, 167 (1981).

[33] A. A. Pivovarov, Nuovo Cimento A **105**, 813 (1992).

[34] W. A. Bardeen, A. J. Buras, D. W. Duke, and T. Muta, Phys. Rev. D **18**, 3998 (1978).

[35] K. G. Chetyrkin, A. L. Kataev, and F. V. Tkachov, Phys. Lett. **85B**, 277 (1979); M. Dine and J. Sapirstein, Phys. Rev. Lett. **43**, 668 (1979); W. Celmaster and R. J. Gonsalves, *ibid.* **44**, 560 (1979); Phys. Rev. D **21**, 3112 (1980).

[36] O. V. Tarasov, A. A. Vladimirov, and A. Yu. Zharkov, Phys. Lett. **93B**, 429 (1980).

[37] W. Celmaster and R. J. Gonsalves, Phys. Rev. D **20**, 1426 (1979); W. Celmaster and D. Sivers, *ibid.* **23**, 227 (1981); A.

Dhar and V. Gupta, Phys. Lett. **B101**, 432 (1981); O. V. Tarasov and D. V. Shirkov, Yad. Fiz. **51**, 1380 (1990).

[38] G. Grunberg, Phys. Lett. **95B**, 70 (1980); Phys. Rev. D **29**, 2315 (1984).

[39] P. M. Stevenson, Phys. Lett. **100B**, 61 (1981); Phys. Rev. D **23**, 2916 (1981).

[40] S. J. Brodsky, G. P. Lepage, and P. Mackenzie, Phys. Rev. D **28**, 228 (1983).

[41] A. Dhar, Phys. Lett. **128B**, 407 (1983); A. Dhar and V. Gupta, Pramāna **21**, 207 (1983); Phys. Rev. D **29**, 2822 (1984).

[42] D. W. Duke and R. G. Roberts, Phys. Rep. **120**, 275 (1985).

[43] C. J. Maxwell, Phys. Rev. D **28**, 2037 (1983).

[44] M. R. Pennington, Phys. Rev. D **26**, 2048 (1982); J. C. Wrigley, *ibid.* **27**, 1965 (1983); P. M. Stevenson, *ibid.* **27**, 1968 (1983); J. A. Mignaco and I. Roditi, Phys. Lett. **126B**, 481 (1983).

[45] R. Marshall, Z. Phys. C **43**, 595 (1989).

[46] Particle Data Group, L. Montanet, Phys. Rev. D **50**, 1173 (1994).

[47] S. L. Adler, Phys. Rev. D **10**, 3714 (1974).

[48] See, for example, S. Narison, Phys. Rep. **84**, 263 (1982).

[49] P. A. Rączka and A. Szymacha (in preparation).

[50] D. E. Soper and L. R. Surguladze, Phys. Rev. D (to be published).